JGP Journal of General Physiology

ARTICLE

ENaC and ROMK channels in the connecting tubule regulate renal K^+ secretion

Lei Yang[1], Yuanyuan Xu[1], Diego Gravotta[2], Gustavo Frindt[1], Alan M. Weinstein[1], and Lawrence G. Palmer[1]

We measured the activities of epithelial Na channels (ENaC) and ROMK channels in the distal nephron of the mouse kidney and assessed their role in the process of K^+ secretion under different physiological conditions. Under basal dietary conditions (0.5% K), ENaC activity, measured as amiloride-sensitive currents, was high in cells at the distal end of the distal convoluted tubule (DCT) and proximal end of the connecting tubule (CNT), a region we call the early CNT (CNTe). In more distal parts of the CNT (aldosterone-sensitive portion [CNTas]), these currents were minimal. This functional difference correlated with alterations in the intracellular location of ENaC, which was at or near the apical membrane in CNTe and more cytoplasmic in the CNTas. ROMK activity, measured as TPNQ-sensitive currents, was substantial in both segments. A mathematical model of the rat nephron suggested that K^+ secretion by the CNTe predicted from these currents provides much of the urinary K^+ required for K balance on this diet. In animals fed a K-deficient diet (0.1% K), both ENaC and ROMK currents in the CNTe decreased by ∼50%, predicting a 50% decline in K^+ secretion. Enhanced reabsorption by a separate mechanism is required to avoid excessive urinary K^+ losses. In animals fed a diet supplemented with 3% K, ENaC currents increased modestly in the CNTe but strongly in the CNTas, while ROMK currents tripled in both segments. The enhanced secretion of K^+ by the CNTe and the recruitment of secretion by the CNTas account for the additional transport required for K balance. Therefore, adaptation to increased K^+ intake involves the extension of robust K^+ secretion to more distal parts of the nephron.

Introduction

The kidneys excrete K^+ into the urine to maintain balance with dietary intake. Proximal nephron segments, especially the proximal convoluted tubule and the ascending limb of Henle's loop, reabsorb most of the K^+ filtered by glomeruli, leaving the distal nephron segments to secrete or reabsorb additional K^+ to match the rate of absorption of the ion from the gut (Malnic et al., 2008). Classical micropuncture experiments done in the 1960s indicated that most K^+ secretion takes place in the distal nephron, including the distal convoluted tubule (DCT) and the downstream connecting tubules (CNTs)—the "micropuncture accessible" portion (Malnic et al., 1964). Widely accepted cellular models for secretion include three essential transport elements. K^+ enters the cells from the interstitial fluid mainly through the Na/K ATPase and exits the cells through apical K^+ channels. Apical Na^+ channels mediate Na^+ entry into the cells from the lumen, stimulating K^+ entry across basolateral membranes by activating the Na^+/K^+ ATPase and K^+ exit into the urine through depolarization of the apical membrane. Apical Na^+ permeability plays a major role in determining the overall rate of K^+ secretion (Weinstein, 2005b; Frindt et al., 2009).

Na^+ channels in the kidney are identified as the epithelial Na channel (ENaC [Scnn1]). They are strongly regulated by the adrenal corticosteroid aldosterone, which is a major determinant of renal K^+ excretion (Garty and Palmer, 1997; Verrey et al., 2008). Indeed, in rats and mice under control conditions (normal rodent chow), ENaC activity is very low in the collecting ducts and CNTs, suggesting minimal K^+ secretory function of those segments (Frindt and Palmer, 2004a; Frindt et al., 2009; Frindt and Palmer, 2010). Recently, however, Nesterov et al. (2012) reported that in more proximal parts of the distal nephron, identified as "DCT2/CNT" segments, ENaC activity is more constitutive and virtually independent of aldosterone. Two types of K^+ channels are found in the apical membranes of distal nephron cells. ROMK channels (Kir1.1, KCNJ1) are thought to be the more important of these under basal conditions, while Ca^{2+}-activated BK channels (KCa1.1, KCNMA1) may be recruited under certain conditions, such as high urine flow rates (Wang et al., 2010; Welling, 2016).

In the present study, we examine both ENaC and ROMK activities along the distal nephron under various levels of

[1]Department of Physiology and Biophysics, Weill-Cornell Medical College, New York, NY; [2]Department of Ophthalmology, Weill-Cornell Medical College, New York, NY.

Correspondence to Lawrence G. Palmer: lgpalm@med.cornell.edu; Y. Xu's present address is Department of Cardiology, The Fourth Hospital of Harbin Medical University, Harbin, China.

dietary K intake. Our overall goal is to evaluate the idea that under basal conditions most K^+ secretion takes place in early segments, while when challenged with additional K^+, more distal segments are recruited to achieve balance between intake and outflow.

Materials and methods

Animals

All procedures using animals were approved by the institutional animal care and use committee of Weill Cornell Medical College. We used adult C57BL/6N mice (20–30 g) of either sex (Charles River). Animals were maintained on chow (Harlan Teklad) containing 0.5% K by weight (control K, TD 99170), 0.05% K (low K, TD07902), or 3% K (high K, TD180098). In the high-K diet, K was added as salts of Cl, carbonate, and citrate in equal molar proportions. Sprague Dawley rats (170–220 g) were maintained on either normal laboratory chow or on a synthetic diet containing 10% KCl.

Electrophysiology

Whole-cell currents were measured in cells of isolated kidney segments containing parts of the DCT and the CNT. After anesthesia, the abdomen and thorax were opened to expose the left kidney, and 5 ml L15 medium (Sigma) containing type 2 collagenase (300 units/ml) was injected through the left ventricle to perfuse the kidney. The renal cortex was separated and cut into small pieces for additional incubation in L15 medium with collagenase for 20–30 min at 37°C to loosen tubular segments. The tissue was washed three times with L15 medium and then kept on ice for manual dissection of DCT/CNT fragments. The tubules were immobilized on a small piece of plastic coverslips (Fisher Scientific) coated with Cell-Tak adhesive (Corning) and transferred to a perfusion chamber on an inverted microscope. The tubules were split open at various points with sharpened micropipettes under the control of a micromanipulator. Seals were formed on the apical surface of principal cells, and whole-cell currents were recorded under voltage-clamp conditions as described previously (Frindt and Palmer, 2004b; Frindt et al., 2009).

Tubules were superfused with solution warmed to 37°C containing (in mM) 135 Na methanesulfonate, 5 KCl, 2 Ca methanesulfonate, 1 $MgCl_2$, 2 glucose, 5 Ba methanesulfonate, and 10 HEPES adjusted to pH 7.4 with NaOH. For ENaC-mediated currents (I_{Na}), pipette solutions contained (in mM) 7 KCl, 123 aspartic acid, 20 CsOH, 20 TEA•OH, 5 EGTA, 10 HEPES, 3 MgATP, and 0.3 NaGDPβS adjusted to pH 7.4 with KOH. I-V relationships were measured before and after addition of 10 µM amiloride to the superfusate. I_{Na} was calculated as the difference in current at a voltage of −100 mV before and during amiloride superfusion. Measurements were accepted only if the I-V curves with and without amiloride converged at positive voltages, indicating a change in Na^+ conductance and not leak conductance. For ROMK-mediated currents (I_{SK}), pipette solutions contained (in mM) 7 KCl, 123 aspartic acid, 5 EGTA, and 10 HEPES adjusted to pH 7.4 with KOH. Cells were held at a clamping voltage of 0 mV, and 100 nM Tertiapin-Q (TPNQ; Sigma) was added to the superfusate. I_{SK} was measured as the decrease in outward current. With no voltage across the cell membrane, leak currents were negligible.

Urinary Na^+ and K^+ excretion

Rats were housed in metabolic cages for the collection of urine. Animals were injected subcutaneously with either TEA chloride (30 µmol/100 g body weight) or with the same volume of isotonic dextrose. Urine was collected over two periods of 60 min. Na and K content was measured using a flame photometer (model 943; Instrumentation Laboratory).

TEA in the urine was measured using liquid ion exchange microelectrodes with a method modified from Cotton et al. (1989). Electrodes were pulled from microhematocrit glass and the tips broken to a diameter of 5–10 µm. Tips were coated by pulling a solution of 4% dichlorodimethylsilane in xylene into the tip. After 10 min, the fluid was expelled from the tip, and the electrodes were baked for 1 h at 100°C. They were filled with 100 mM KCl using suction. The final 2 mm of the tip was exchanged with K-selective ion exchange resin (5% tetraphenylborate in 3-o-methylxylene).

Microscopy

Tubules were prepared as for electrophysiology, with the addition of cycloheximide (100 µg/ml) to the L15 solution. Dissected tubules were attached to coverslips and fixed for 30 min in PBS with 4% paraformaldehyde on ice. This was followed by two 10-min washes with PBS and incubation in PBS with 50 mM ammonium acetate for 20 min at room temperature. After a wash with PBS, the tubules were permeabilized for 10 min in fresh 0.1% saponin in PBS and blocked with 1% IgG-free albumin in PBS for 30 min. Samples were incubated with the primary antibodies at 4°C overnight in PBS with 1% albumin. The primary antibodies were a polyclonal rabbit antibody raised against a C-terminal epitope of βENaC (Ergonul et al., 2006) diluted 1:150 and a guinea pig polyclonal antibody raised against an N-terminal epitope of mouse Na–Cl cotransporter (NCC): NH2-LPGEPRKVRPT-LADLH-COOH (Dimke et al., 2011) diluted to 2 µg/ml (a gift from Prof. Johannes Loffing, University of Zürich, Zürich, Switzerland). Tubules were then washed four times for 10 min each with PBS + 1% albumin. Bound primary antibodies were visualized with secondary Alexa Fluor 568 or 488 conjugated to cross-absorbed goat antibodies (Life Technologies) at room temperature for 1 h and washed four times with PBS + 1% albumin. Finally, they were mounted in DAPI-VECTASHIELD.

Distal tubules were examined with a Zeiss Cell Observer SD confocal microscope equipped with a Yokagawa CSU-X1 spinning disk, a Plan-Apochromat 63×/1.4 M27 oil-immersion objective paired with a 1.2× adapter to a Photometrics, and an Evolve 512 electron multiplying charge-coupled device camera. Image stacks were collected by Nyquist sampling and by using identical settings across samples. Rotations and 3-D renderings were generated by processing Z-stack images using ZEN v3.5 software (Carl Zeiss MicroImaging).

The fluorescence images for each tubule segment encompass five consecutive fragments scanned under identical conditions. Quantification of the fluorescence signal was performed with

ZEN imaging software (Zeiss). Image stacks (~220 slices) were marked with a region of interest to delineate the tubule. Thresholds were set before retrieving the number of pixels (Pn) and mean intensity (Mi) per slide in each channel (channel 1, 488-label; channel 2, 568-label). The segment fluorescence (Sf) is calculated as the sum of the product of Pn and Mi in each slice: Sf = (Pn × Mi).

Modeling

The numerical models of rat kidney used in these calculations are based on those of prior work (Weinstein, 2005a, b). In the original model, the perfused DCT/CNT consisted of two 1-mm segments. For the calculations of this study, the true DCT was shortened to 0.75 mm, and all luminal membrane Na^+ channel activity was eliminated so that the only pathways for luminal Na^+ entry are NCC and Na–H exchanger (NHE2). Otherwise, the transport parameters for this segment are as published. A 0.25-mm early CNT (CNTe) was fashioned by starting with DCT, adding a luminal Na^+ conductance, and augmenting the luminal K^+ conductance in accordance with the measurements from this study. The length of the segment was chosen to approximate that in which constitutive ENaC activity was measured in the mouse tubule. The aldosterone-sensitive CNT segment (CNTas) is as published, with several modifications: In prior models, the representation of luminal membrane Na^+ permeability ($H_{MI}(Na)$) included terms for both luminal self-inhibition and cytoplasmic feedback inhibition that had been developed for ENaC:

$$H_{MI}(Na) = H_{MI0}(Na)\left[\frac{1 - C_I(Na)/K_I}{1 + C_M(Na)/K_M}\right],$$

where luminal and cytoplasmic Na^+ concentrations C_M and C_I are scaled according to K_M = 30 mM and K_I = 5 mM. In the current work, K_M = 10 mM to reflect the determination by Palmer et al. (1998). All the CNT tight junction permeabilities have been reduced by a factor of 5 so that the simulations reflect the maximal capacity of the segment to drive K^+ secretion. Luminal conductances for Na^+ and K^+ were taken in accordance with measurements from this study. To determine suitable coefficients for the cell luminal membrane Na^+ and K^+ permeabilities, simulations were done in which model tubules were perfused at 60 nl/min, using Na^+ = 145 mM and K^+ = 2.0 mM, comparable to the experimental perfusate. Then, the model permeabilities, $H_{MI0}(Na)$ and $H_{MI0}(K)$, were selected to achieve agreement with the measured cellular fluxes of Na^+ and K^+ in CNTe and CNTas. The parameters shown in Table 1 are for $H_{MI0}(Na)$ of the equation above and for $H_{MI0}(K)$, which scale their respective Goldman formulas representing the luminal membrane fluxes. In the absence of measurements for CNTas principal cells with the low-K diet, control diet parameters were used.

Data analysis

Statistical analysis used GraphPad Prism 9. Analysis of electrophysiological data used nested analysis in which cells from the same animal were grouped. Statistical significance was evaluated using either an unpaired two-tailed *t* test or ANOVA with Dunnett's posttest for multiple comparisons. P values are indicated in the figures where appropriate.

Table 1. **Luminal membrane permeability assignment for Na^+ and K^+ permeabilities**

	CNTe		CNTas	
	Na^+	K+	Na^+	K+
Control				
Whole-cell current (pA/cell)	660	−430	30	−260
Luminal fluxes (fmol/cell)	6.8	−4.5	0.3	−2.7
Epithelial fluxes (nmol/s/cm^2)[a]	6.1	−3.9	0.3	−2.4
H_{MI0} (cm^3/s/cm^2 epithelium) × 10^5	16.5	2.8	0.13	1.8
High-K diet				
Whole-cell current (pA/cell)	770	−1,250	480	−780
Luminal fluxes (fmol/cell)	8.0	−13.0	5.0	−8.1
Epithelial fluxes (nmol/s/cm^2)[a]	7.1	−11.5	4.4	−7.2
H_{MI0} (cm^3/s/cm^2 epithelium) × 10^5	24.9	8.5	2.2	5.3
Low-K diet				
Whole-cell current (pA/cell)	360	−180		
Luminal fluxes (fmol/cell)	3.7	−1.9		
Epithelial fluxes (nmol/s/cm^2)[a]	3.3	−1.7		
H_{MI0} (cm^3/s/cm^2 epithelium) × 10^5	8.5	1.2	0.13	1.8

Assumes 500 cells/mm of tubule and tubular inner diameter of 18 µm.
[a]Transcellular fluxes refer to epithelial area.

Online supplemental material

Fig. S1 shows immunocytochemical localization of βENaC in segments S2–S4 of the DCT/CNT of four mice on control Na diets.

Results

Control K diet

ENaC activity

Fig. 1 A shows a photomicrograph of a distal nephron fragment, illustrating its subdivision into various regions. The DCT is recognized by the convolutions and, in favorable cases, by an attached thick ascending limb and/or glomerulus. The tubule eventually straightens and narrows abruptly at a point considered to represent the junction between the DCT2 and the CNT (Nesterov et al., 2012; Wu et al., 2018). We opened the tubule at various points along its length, both proximal and distal to this narrowing, and made whole-cell recordings under conditions favorable to the detection of ENaC currents. After recording currents in response to changes in clamping voltage, amiloride (10^{-5} M) was added to the superfusate, and the currents were re-recorded with the same pulse protocol.

Results are illustrated in Fig. 1, B and C. All cells studied showed large currents attributable to Cl^- channels (Palmer and Frindt, 2006). These currents declined with time after the

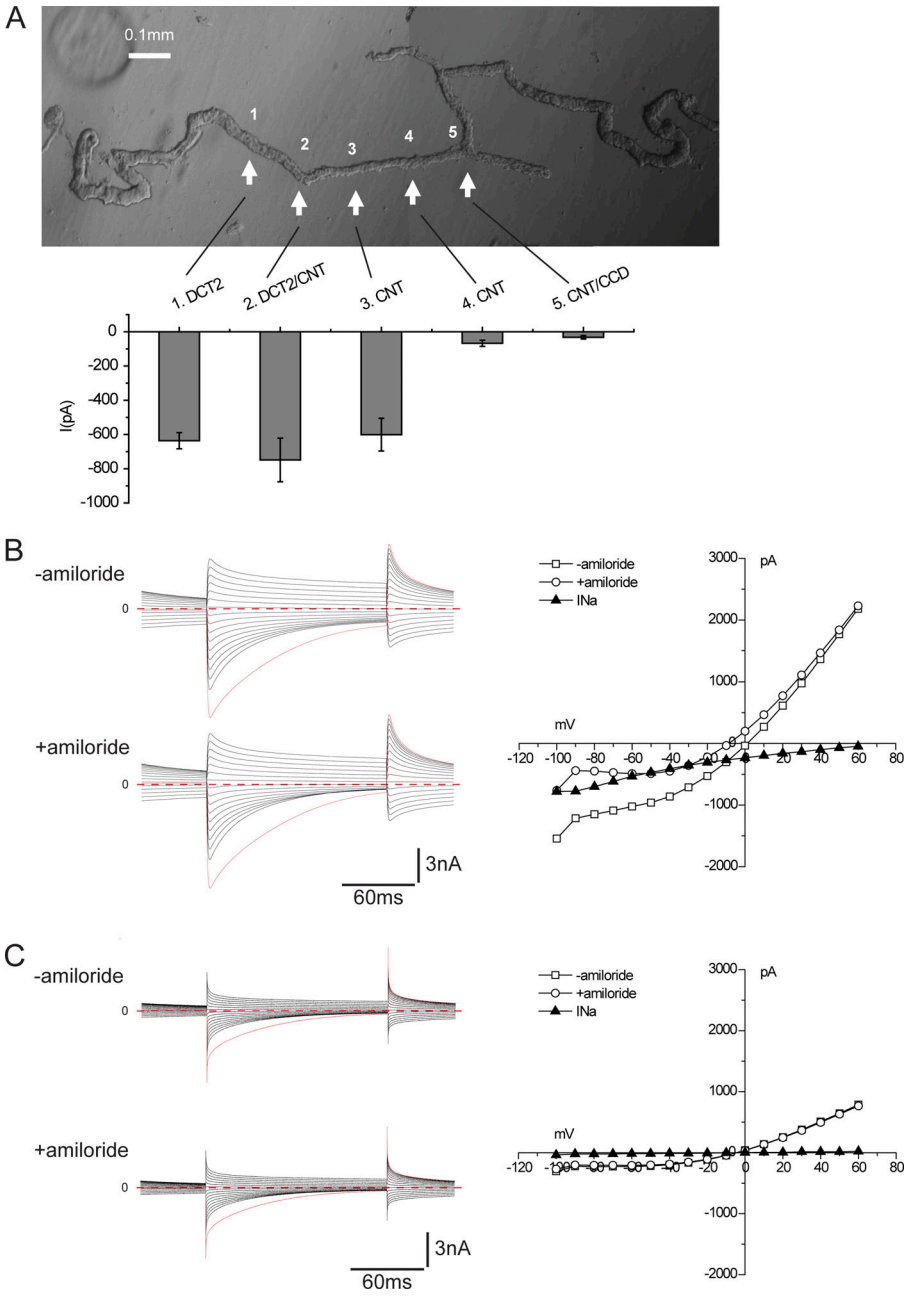

Figure 1. **ENaC activity along the distal nephron under control conditions.** Mice were fed a diet containing 0.5% K for 6–8 d. **(A)** The composite micrograph shows an isolated fragment containing two DCT segments with corresponding CNTs. The arrows indicate five regions of the fragments selected for electrophysiological analysis after being split to expose the luminal membrane. The bar graph indicates mean values of amiloride-sensitive currents in these regions in mice fed a control diet. Data represent mean ± SEM for 18, 17, 34, 29, and 17 cells, respectively, from four (DCT2, DCT2/CNT) or six (CNT, CNT/CCD) different animals. **(B)** ENaC currents under whole-cell voltage-clamp conditions in a cell from region 2. Currents were measured at the end of a voltage pulse of 150 ms in the presence and absence of 10 µM amiloride. The amiloride-sensitive current (I_{Na}) was calculated as the difference in currents at a voltage of −100 mV. **(C)** ENaC currents under whole-cell voltage-clamp conditions in a cell from region 4. There was no detectable response to amiloride in this cell.

voltage change, particularly in the inward direction, related at least in part to unstirred layer effects (Palmer and Frindt, 2006). In a cell from region 2 close to the putative DCT/CNT junction, inward, amiloride-sensitive currents (I_{Na}) characteristic of ENaC, with reversal potentials >60 mV, were superimposed on the Cl^- currents (Fig. 1 B). In a cell from region 5 close to the branch point, the Cl^- currents were lower in magnitude, and the Na^+ currents were virtually absent (Fig. 1 C). The bar graph in Fig. 1 A shows the average magnitude of I_{Na} at different positions. These currents were large near the change in tubule diameter (region 2) and in the adjacent regions 100–150 µm proximal (region 1) and distal (region 3) to the diameter change. They decreased abruptly in the distal direction and were almost undetectable at or beyond the middle of this segment. These results confirm and extend those of Nesterov et al., (2012).

Immunocytochemistry

To further characterize differences in this part of the distal nephron, we used immunocytochemistry to probe for expression of NCC, a defining marker of the DCT, and ENaC. Nephron fragments were isolated from collagenase-treated mouse kidney cortex as for electrophysiology, fixed, and stained with antibodies against βENaC and NCC. Fig. 2 shows typical staining patterns for five contiguous segments of the same preparation, each ~150 µm in length, starting at the point of contact with the glomerulus. These were made independently of the divisions used for electrophysiology. Measurements of tubule diameter showed an abrupt narrowing between S3 and S4, suggesting that these conform most closely with positions 2 and 3 in Fig. 1. Toward the proximal end, NCC expression dominates, with little ENaC discernible. The opposite pattern occurs at the distal end

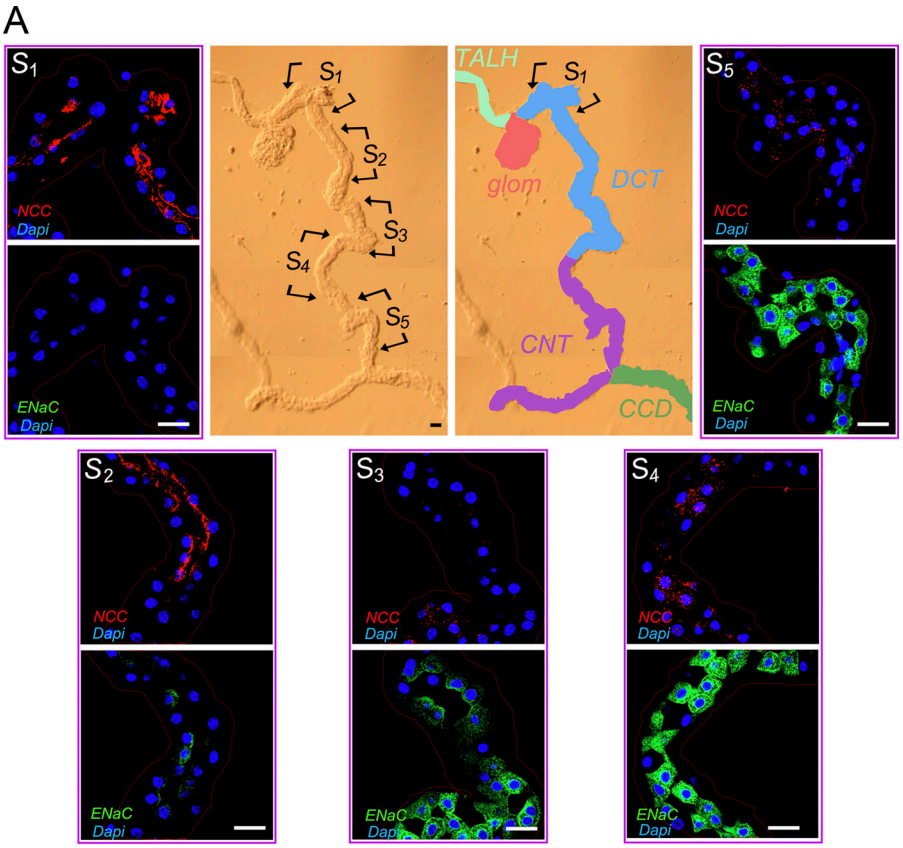

Figure 2. **ENaC protein expression along the distal nephron. (A)** Center: A bright field image of an isolated fragment from mouse kidney together with the designation of anatomically defined segments. The image was divided into five regions (S1–S5) for confocal fluorescent imaging showing ENaC (green), NCC (red), and DAPI nuclear (purple) signals. Little ENaC is expressed in S1, the region with the highest NCC signal. ENaC is seen mostly at the apical pole in regions S2 and S3. In S4 and S5, ENaC is distributed broadly within the cytoplasm. Scale bars, 10 µm. **(B)** Quantitation of ENaC and NCC abundance. For each region, signals were normalized to the total intensity along the entire segment. Mean tubule diameter along the tubules (blue) was also measured. P values indicate significance of differences from S5 (red) or from S1 (blue, green). Data represent mean ± SEM for seven tubules from seven different animals.

with high ENaC and low NCC staining. The middle segments show some coexpression of the two proteins, although the overlap, quantified in Fig. 2 B, was minimal. Intercalated cells, which do not stain with either antibody, start to appear at the center of segment 3.

In addition to changes in overall ENaC abundance along the nephron, we noted differences in its subcellular distribution. In regions 2 and 3 at or near the presumed DCT/CNT junction, much of the channel protein resides near the apical membrane, while in the more distal parts of the CNT it has a more diffuse cytoplasmic location. Other examples are shown in Fig. S1. Previous studies in the CNT and cortical collecting duct (CCD) showed migration of ENaC from perinuclear regions toward the apical pole under conditions of elevated aldosterone (Masilamani et al., 1999; Loffing et al., 2000b; Loffing et al., 2001b). In one of those studies (Loffing et al., 2000b), ENaC in the late DCT had a more apical distribution under control conditions, consistent with our observations. It is therefore likely that the constitutive ENaC currents in this part of the nephron arise in part from aldosterone-independent trafficking of channel subunits to the apical surface. Because part of this segment with apical expression occurs in the absence of significant NCC expression, we have opted to call it CNTe rather than DCT2 since the latter term implies the presence of NCC.

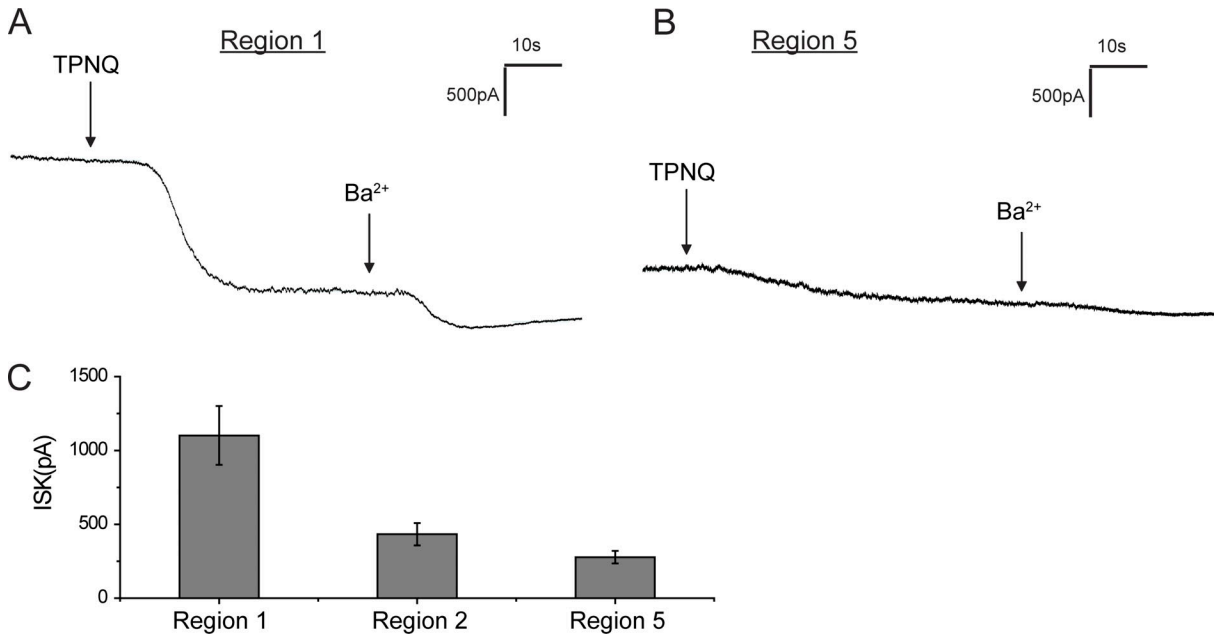

Figure 3. **ROMK currents along the distal nephron under control conditions. (A and B)** Whole-cell currents were continuously measured at a voltage of 0 mV during addition of TPNQ (0.1 µM) and Ba^{2+} (5 mM) to the superfusate in region 1 and region 5 (see Fig. 1 A). **(C)** The currents through ROMK channels (I_{SK}) were assessed as the decrease in outward current with TPNQ and are shown as mean ± SEM for 23, 16, and 22 cells, respectively.

This portion of the renal tubule is therefore defined functionally as having constitutive ENaC activity. It includes the anatomically defined DCT2. We refer to the more distal parts of the CNT in which ENaC activity depends on aldosterone as the CNTas portion.

ROMK activity

To secrete K^+, the cells also need apical K^+ channels to mediate electrogenic exit of the ion from the cell into the lumen. ROMK is one such channel, recognizable from its sensitivity to the bee venom TPNQ. To see whether the segments with constitutive ENaC activity also have conducting ROMK channels, we measured outward currents at a constant holding potential of 0 mV before and after the application of TPNQ (10^{-7} M). Fig. 3 shows typical traces from cells of the CNTe (Fig. 3 A) and CNTas (Fig. 3 B). In both cases, the ROMK currents were easily measurable, although they were considerably larger in the CNTe (Fig. 3 C). With this protocol, the TPNQ-insensitive K^+ currents through basolateral channels run down while TPNQ-sensitive currents are relatively stable (Frindt et al., 2009). These currents are therefore artificially low and were not quantified.

Role of BK channels

In addition to ROMK channels, high-conductance BK channels may play a role in K^+ secretion, especially at high urine flow rates or with dietary K loading (Pluznick and Sansom, 2006). To test for a role of these channels in overall K^+ secretion, we assessed effects of TEA in vivo. TEA is a moderately selective blocker of BK channels with a K_I of ~0.2 mM (Yellen, 1984; Frindt and Palmer, 1987; Lang and Ritchie, 1990). It is a convenient reagent for this purpose because it is avidly secreted by the proximal tubule, increasing its concentration in downstream, K^+-secreting segments. Previous studies showed that most TEA injected into rats is cleared in the urine within 1 h (Jonker et al., 2003).

TEA in the urine was measured using K^+-selective liquid ion exchanger electrodes (Palmer and Civan, 1977; Cotton et al., 1989). A calibration curve is illustrated in Fig. 4 A. The response to TEA was consistently super Nernstian. In four rats, TEA concentrations in the urine during the first hour of collection ranged from 11.2 to 17.1 mM. These numbers account for 46 ± 11% of the injected TEA. Combining three collection periods of 1 h each, 74 ± 8% of the injected drug was excreted. To estimate the concentration of TEA in the fluid at the end of the DCT, we assumed a glomerular filtration rate of 1 ml/min and a delivery of 20% of filtered fluid to the distal nephron (Frindt and Palmer, 2009). We further assumed no addition or removal of TEA from the tubular fluid between the DCT and the final urine. This gave estimates of 1.1–1.5 mM (mean, 1.3 mM), approximately six times the expected K_I for BK channels.

As shown in Fig. 4 B, urinary Na^+ and K^+ excretion was not affected by TEA administration under control conditions. We also increased K^+ excretion in two ways. First, rats were fed a diet containing 5% K for 7 d, increasing K^+ excretion approximately threefold without changing Na^+ excretion. Second, furosemide injection (6 mg/kg body weight) increased Na^+ and K^+ excretion simultaneously (Fig. 4 B). Under these conditions TEA still had no effect on excretion of either ion. We conclude that under the conditions used in this paper, K^+ secretion through BK channels plays a minor role in maintaining K^+ balance.

Simulations

The mathematical model of DCT-CNTe-CNTas was used to simulate tubule perfusion at a physiological flow rate (6 nl/min),

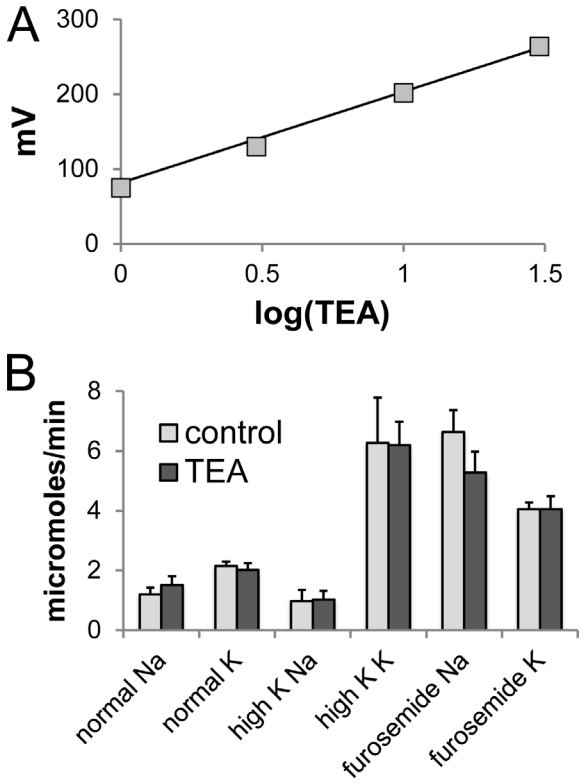

Figure 4. **Effect of TEA on urinary Na^+ and K^+ excretion in the rat. (A)** Calibration of TEA-sensing electrodes. Electrodes were filled with 100 mM KCl. The test solution contained 100 mM KCl + 1–30 mM TEA•Cl. The regression line represents V = 130•log(TEA) + 73. **(B)** Na and K excretion during the first hour after administration of TEA (30 µmol/100 g body weight) or vehicle. Data represent mean ± SEM for six to seven measurements in rats under control conditions, with dietary K loading for 7 d, or after administration of furosemide (6 mg/kg body weight).

with a fluid composition characteristic of early DCT (Na^+ = 65 mM and K^+ = 2.0 mM, as in Table 5 of Weinstein, 2005a). The three calculations correspond to model parameters identified for baseline, high-K, and low-K animals (Table 1). In Table 2, segmental flows and fluxes of volume, Na^+, and K^+ are displayed, and Fig. 5 illustrates the axial profiles of volume and solute under these conditions. The DCT (0–0.75 mm) shows robust Na^+ reabsorption, mainly through NCC and the NHE2. Volume reabsorption is minimal due to a low H_2O permeability. Transepithelial voltage is small and lumen positive, reflecting the lack of electrogenic luminal Na^+ entry. There is a slow addition of K^+ to the luminal fluid, 75% of which is attributable to the inclusion of a K–Cl cotransporter in the luminal membrane. Secretion through ROMK channels is only a small fraction of this slow rate, indicating the requirement for the electrical driving force provided by ENaC activity for secretion through apical K^+ channels in these cells. The CNTe segment (0.75–1 mm) secretes K^+ more vigorously due to the presence of ENaC activity, adding 9 pmol/min to the urine. The K–Cl cotransporter is also assumed to operate at similar rates in the CNTe, but here the rate of secretion is a small (~10%) fraction of the total. Under control conditions, there is no further downstream K^+ secretion due to the absence of ENaC activity, and indeed, the model predicts K^+

Table 2. **Segmental flows and fluxes of volume, Na^+, and K^+**

	DCT	CNTe	CNTas	End/ total
Control				
Absolute delivery				
Fv (nl/min)	6.0	5.6	5.4	2.6
Na^+ (pmol/min)	390.0	274.1	231.8	221.9
K^+ (pmol/min)	12.0	16.5	25.1	16.9
Absolute reabsorption				
Fv (nl/min)	0.4	0.2	2.8	3.4
Na^+ (pmol/min)	115.9	42.3	10.0	168.1
K^+ (pmol/min)	−4.5	−8.6	8.3	−4.9
Reabsorption relative to DCT delivery				
Fv (%)	7.3	2.7	47.3	57.2
Na^+ (%)	29.7	10.9	2.6	43.1
K^+ (%)	−37.5	−72.0	69.0	−40.5
High-K				
Absolute delivery				
Fv (nl/min)	6.0	5.6	5.4	2.4
Na^+ (pmol/min)	390.0	274.1	222.5	150.1
K^+ (pmol/min)	12.0	16.5	32.8	60.7
Absolute reabsorption				
Fv	0.4	0.2	3.0	3.6
Na^+	115.9	51.6	72.5	239.9
K^+	−4.5	−16.3	−27.8	−48.7
Reabsorption relative to DCT delivery				
Fv (%)	7.3	2.7	49.3	59.2
Na^+ (%)	29.7	13.2	18.6	61.5
K^+ (%)	−37.5	−136.0	−232.0	−405.5
Low-K				
Absolute delivery				
Fv (nl/min)	6.0	5.6	5.4	2.6
Na^+ (pmol/min)	390.0	274.1	237.1	226.5
K^+ (pmol/min)	12.0	16.5	20.3	13.6
Absolute reabsorption				
Fv	0.4	0.2	2.8	3.4
Na^+	115.9	37.0	10.6	163.5
K^+	−4.5	−3.8	6.7	−1.6
Reabsorption relative to DCT delivery				
Fv (%)	7.3	2.7	47.2	57.1
Na^+ (%)	29.7	9.5	2.7	41.9
K^+ (%)	−37.5	−31.5	55.5	−13.5

Fv, volume flow.

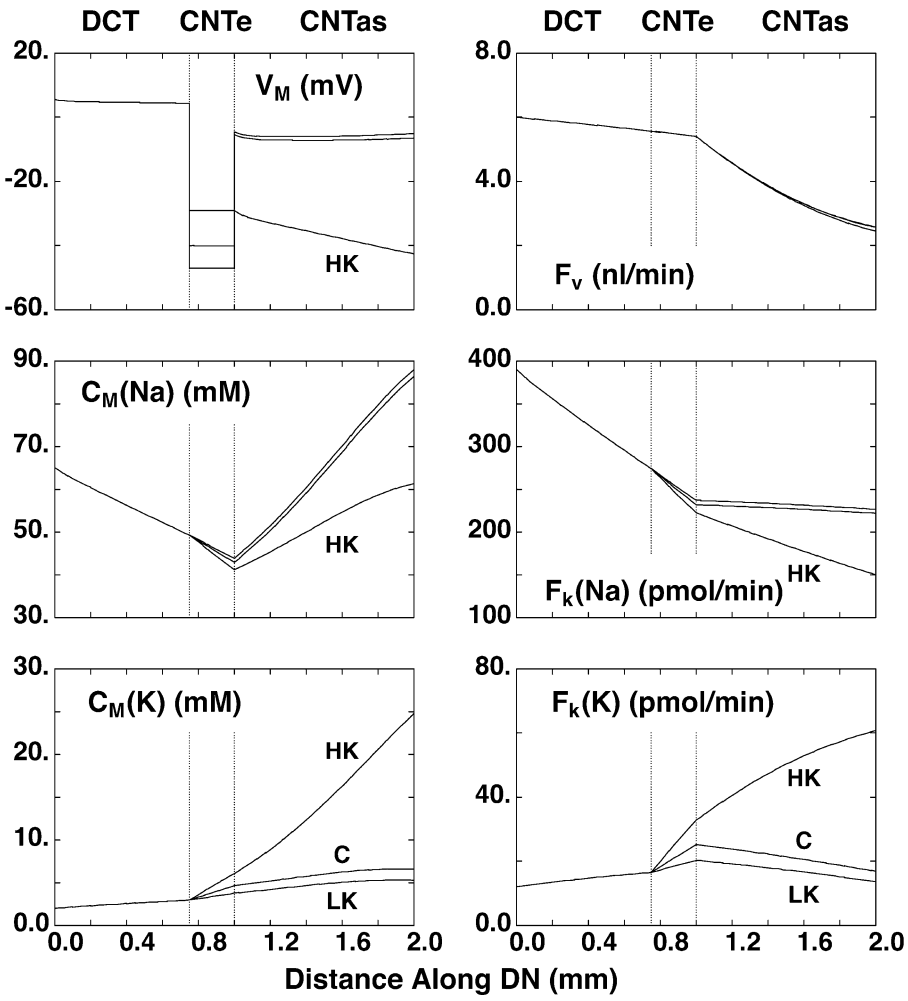

Figure 5. **Simulation of transport along the distal nephron.** A mathematical model of the rat DCT-CNTe-CNTas was used to calculate expected Na^+ and K^+ transport using apical Na^+ and K^+ permeabilities measured under control (C), low-K (LK), and high-K (HK) conditions. Panels show transepithelial voltage (V_M), luminal concentrations of Na^+ (C_M(Na)), and K^+ (C_M(K)) and flows of volume (F_v), Na^+ (F_k(Na)), and K^+ (F_K(K)) along the nephron. The segment labeled as DCT corresponds most closely with DCT1 as defined anatomically.

reabsorption by the CNTas, as luminal solutes are concentrated due to water reabsorption. Micropuncture studies in the rat indicated ~50% K^+ reabsorption between CNT and the final urine, when animals were antidiuretic (Fig. 3 in Malnic et al., 1964). With 72,000 nephrons/two kidneys (Knepper et al., 1977), the 9 pmol/min from the CNTe translates to 0.65 µmol/min delivered to the urine in the absence of further collecting duct reabsorption. We previously measured excretion rates of 0.8 µmol/min in rats under similar conditions, nearly all of which was blockable by amiloride (Frindt and Palmer, 2009). Factors that may account for the discrepancy between the model estimate and whole-rat data include the possibility that luminal flows are >6 nl/min in vivo, that the CNTe region may be longer in rats, and that the tubules sampled reflect superficial nephron fluxes, which may be half those of juxtamedullary nephrons.

The calculations of Fig. 6 are done using the model of the open-circuited CNTe epithelium, in which luminal and peritubular bathing conditions are fixed, and examine the impact of having both ENaC and NCC active in the same cell, the defining property of DCT2. The abscissa for each pane is the apical Na^+ permeability, which is varied over the range measured for the CNTe; other transporters are kept constant. Activation of ENaC increases overall Na^+ transport, with fluxes saturating at the highest permeability levels. Transport through NCC and NHE2 is reduced only slightly. The apical membrane voltage depolarizes, increasing the driving force for K^+ secretion. These results indicate that ENaC/ROMK and NCC/NHE2 systems can operate almost independently in cells where both are present.

Low-K diet

Channel activity

When animals eat a K-restricted diet, K^+ secretion is reduced, and the distal nephron switches to K^+ reabsorption (Malnic et al., 1964). We examined channel activity in the CNTe isolated from mice fed a low-K (0.1% K) diet for 5–6 d. Fig. 7 illustrates that both ENaC and ROMK currents were reduced under these circumstances. As shown in Fig. 8, mean I_{Na} levels fell by 45% relative to control K, although this was not significant by ANOVA. The currents from low-K animals were significantly lower than in the combined populations of high-K and control-fed mice (P = 0.04), suggesting that ENaC can be regulated by K intake in this part of the nephron. Mean I_{SK} levels declined by 60% relative to the control diet.

Simulations

Using the mathematical model, we calculate that the CNTe segment will add 3.8 pmol/min under these low-K condition (Table 2 and Fig. 5). Although this is significantly (60%) lower

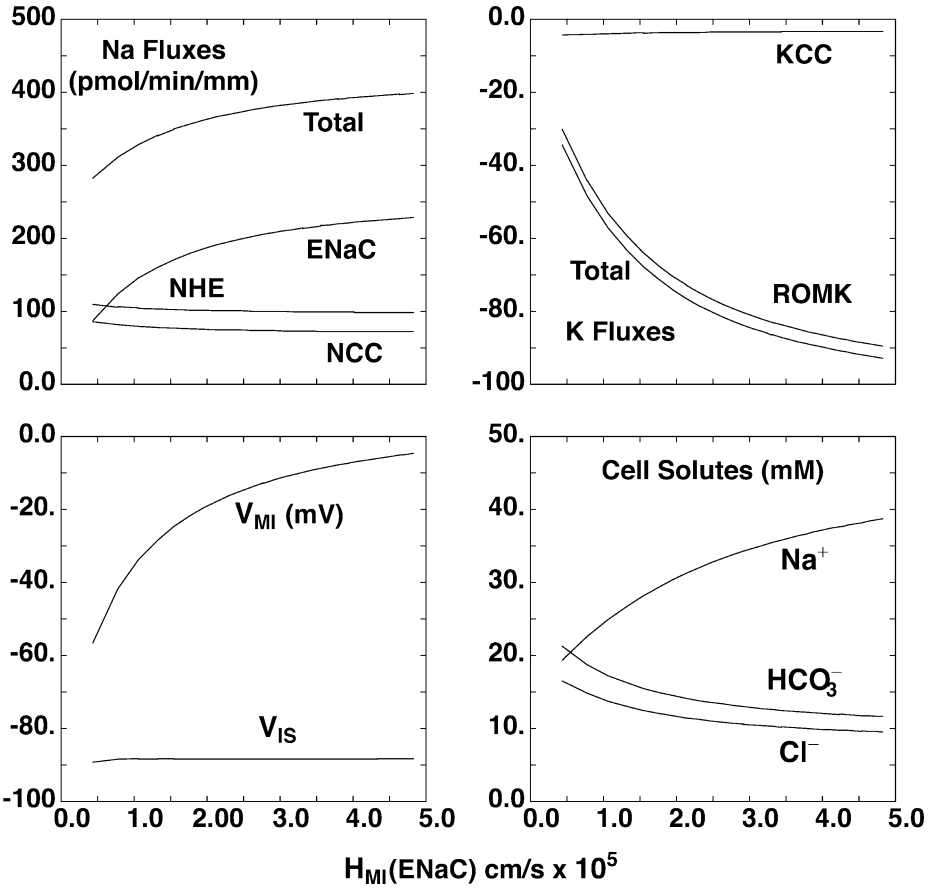

Figure 6. **Simulation of transport in a segment with both NCC and ENaC in the luminal membrane.** We started with a mathematical model of the rat DCT epithelium corresponding to DCT1. This was used to calculate expected Na^+ and K^+ transport using fixed NCC activity and apical K^+ permeability as apical Na^+ permeability (H_{MI}(ENaC)) was increased, as expected for the DCT2 segment. The panels show Na fluxes through ENaC, NCC, and NHE; K fluxes through ROMK and K–Cl cotransporter (KCC); apical (V_{MI}) and basolateral (V_{IS}) membrane voltage; and cell solute concentrations. Na^+ reabsorption through NCC and NHE is largely independent of ENaC activity. K^+ secretion depends almost entirely on the presence of ENaC to depolarize the apical membrane.

than the value under control conditions, it does not fully account for the overall decrease in K^+ excretion, which falls by ∼90% (Malnic et al., 1964). This illustrates the need for the activation of a K^+ reabsorption mechanism in the distal nephron and/or collecting ducts to minimize urinary K^+ losses.

High-K diet

Channel activity

We next repeated measurements of channel activity in tubules from mice fed a diet enriched in K (3%) for 6–8 d. Under these conditions, the kidney secretes more K^+ to balance the increased intake of the ion. Fig. 9 shows ENaC currents in the CNTe and in more distal CNT regions under these conditions. In the CNTe, these currents were similar to those under control conditions, increasing by only ∼15%. In contrast, in the more distal regions (CNTas), I_{Na} increased from almost undetectable levels to magnitudes that approach those of the CNTe. Since high K intake stimulates secretion of aldosterone by the adrenal cortex, this is consistent with the idea that ENaC is aldosterone dependent in the late CNT but aldosterone independent in the CNTe (DCT2/CNT; Nesterov et al., 2012). However, the latter segment still responded to increased K^+ intake. ROMK currents increased by approximately threefold in both the CNTe and the CNTas in animals fed with the high-K relative to the control diet (Fig. 10). Overall, these K^+ currents varied >10-fold between extremes of dietary K intake.

Simulations

The mathematical model predicts that K^+ secretion in the CNTe increases from 9 to 16 pmol/min under high-K conditions (Table 2). However, the largest changes in permeabilities took place in the CNTas, which now adds additional K^+ to the urine. As shown in Fig. 5, K^+ secretion, now all along the CNT, adds 28 pmol/min to the urine. Thus, when referred to all 72,000 nephrons, the ENaC-dependent portion of secretion increases from 0.5 to 4.2 µmol/min, which compares well with the increase in amiloride-sensitive K^+ excretion from 0.8 to 3 µmol/min (Frindt and Palmer, 2009) for rats eating a high-K diet. Thus, the simulations suggest that the measured permeabilities can account for a physiologically significant K^+ secretion in K-loaded as well as in control animals. Of note, to maintain this level of net K^+ secretion in the CNT, it was necessary to increase the paracellular resistance in this segment from 120 Ω•cm² to 600 Ω•cm². With the lower resistance, significant amounts of

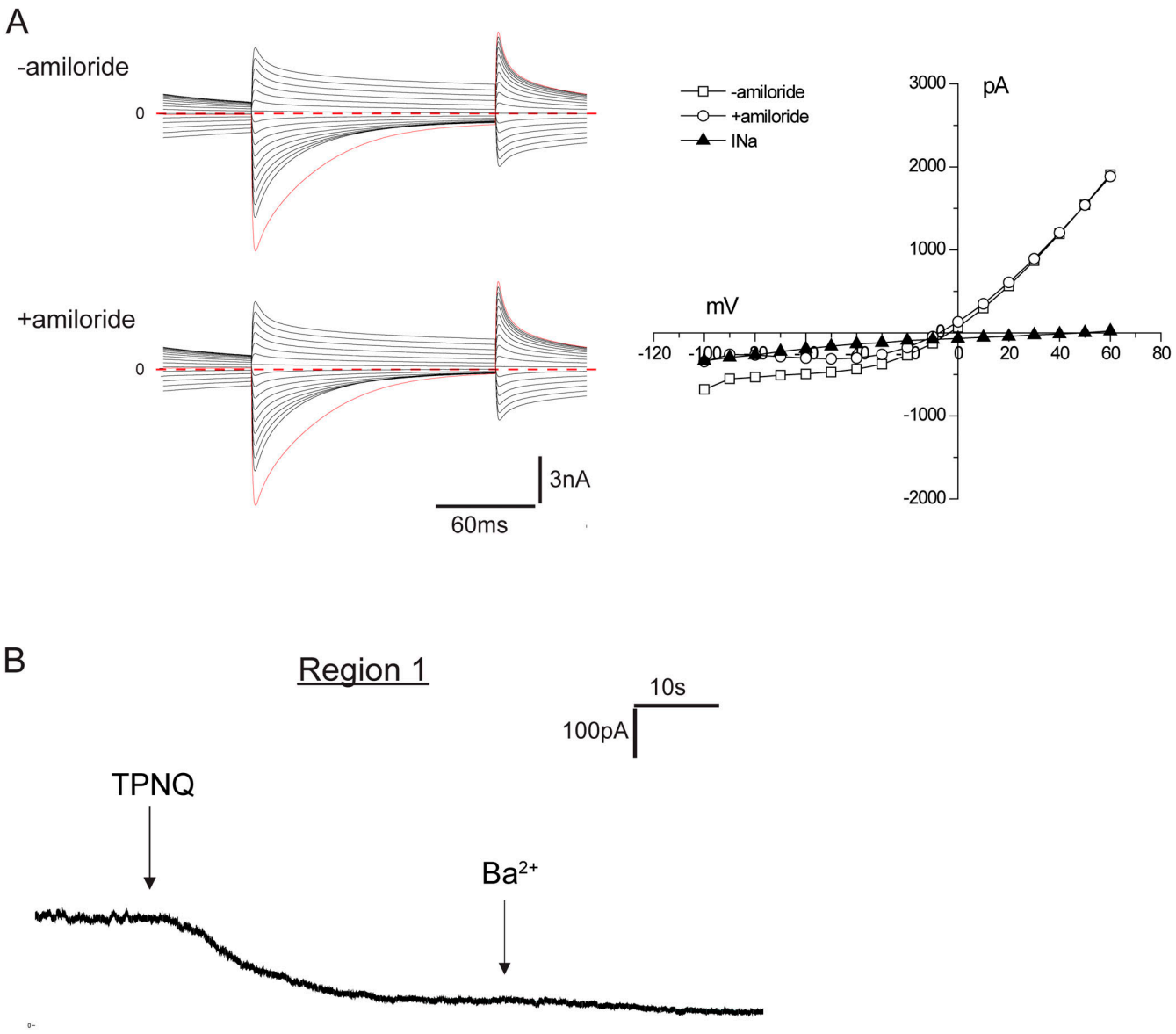

Figure 7. **ENaC and ROMK currents under low-K conditions.** Mice were fed a diet containing 0.05% K for 5–6 d. **(A)** Currents in the absence and presence of amiloride in a cell from region 2. I–V relationships were used to calculate the difference currents (I_{Na}). **(B)** Currents at 0 mV before and after sequential addition of TPNQ and Ba^{2+} to the superfusate.

secreted K^+ are reabsorbed through the tight junctions. We know of no direct measurements of this parameter in the CNT.

Discussion

ENaC activities along the nephron

In the kidney, ENaC has classically been considered to be tightly regulated by the adrenal corticosteroid aldosterone. Nesterov et al. (2012) first reported constitutive ENaC activity that is independent of aldosterone in the mouse distal nephron. They compared two regions: one near the junction between the DCT and the CNT that had high ENaC currents under both control and Na-depleted conditions and a second near the junction between the CNT and the CCD where currents increased dramatically with Na depletion. The findings were confirmed by Wu et al. (2020), who reported that DCT/CNT cells were more sensitive than those of the CCD to changes in angiotensin II signaling. ROMK currents have also been observed in this segment, and their activity is increased in animals fed a K-rich diet (Zhang et al., 2017; Wu et al., 2018).

We confirmed these findings and extended them in several ways. We showed that in mice on a control diet (0.5% K), the constitutive activity extended ∼100 µm from the presumed DCT/CNT junction (assessed by tubule morphology) into more proximal parts of the nephron. Going more distally, this activity continued a small distance but essentially disappeared in the central portion of the CNT. This suggests a fairly abrupt transition from constitutive to highly regulated ENaC. This part of the distal nephron is close to that called the DCT2, which is defined by the expression of the DCT marker NCC together with

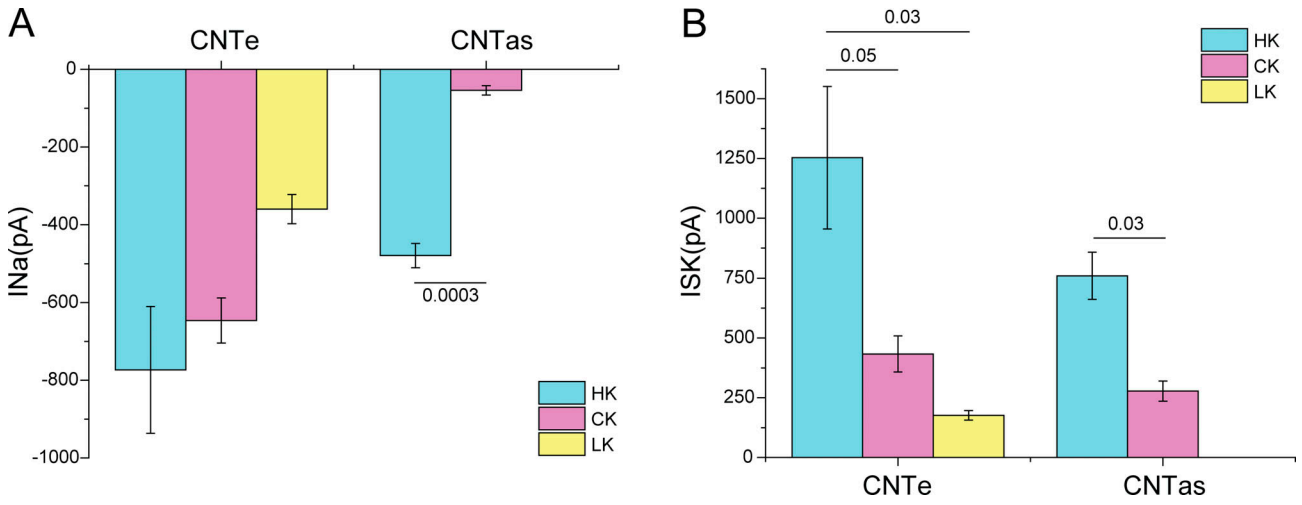

Figure 8. **Mean values of I_{Na} and I_{SK} in the CNTe (regions 1–3) and the CNTas (region 4) in mice on control-K, low-K, and high-K diets.** Data represent mean ± SEM for 11–49 cells from four to eight separate animals (I_{Na}) and from three to seven animals (I_{SK}). P values indicate comparisons of high-K with control-K or low-K diets using *t* tests (CNTas) or ANOVA (CNTe).

ENaC and Ca transport proteins (Loffing et al., 2001a). We prefer the term CNTe for the region with constitutive ENaC activity for several reasons. First, this activity extends distally beyond the morphological transition thought to represent the DCT2/CNT boundary (Fig. 1). Second, the parts of the nephron where we measured this activity were relatively straight and lacked convolutions at least in the isolated fragments. Third, some parts of this region lack significant NCC expression but have ENaC expressed at the apical pole of the cell under control conditions, suggesting constitutive activity (Fig. 2). Finally, some species, such as the rabbit, appear to lack the DCT2 segment (Loffing et al., 2000a). The use of the term CNTe could include a constitutive Na^+-reabsorbing, K^+-secreting segment in those kidneys.

We also assessed the effects of dietary K intake on ENaC activity. In the CNTe, currents increased modestly—by ∼20%—when the K content increased from 0.5 to 3% and decreased by 45% when the K content was lowered to 0.05%. Altogether, there was a twofold change of activity. This was statistically significant and indicates that the channels are regulated by dietary K in this segment. We do not know what signaling pathways mediate these changes, but they are presumably independent of aldosterone. The differences in the CNTas were much larger. In these segments I_{Na} was absent in many cells and small in the rest under control conditions but increased to levels comparable to those of the CNTe when K intake was high. This effect is presumably due, at least in part, to increases in circulating aldosterone levels.

Immunocytochemical images suggested that ENaC protein trafficking represents one difference in the control of channel activity in the CNTe and CNTas. In the CNTas under control conditions, most ENaC is distributed diffusely in the cytoplasm, in agreement with many previous reports (Masilamani et al., 1999; Loffing et al., 2000b; Loffing et al., 2001b). With elevations in aldosterone, much of the protein migrates toward the apical membrane. In contrast, in the CNTe, most ENaC is near the apical pole of the cells, even under control conditions (Fig. 2). A similar observation was reported previously (Loffing et al., 2000b).

The reasons for the differences in aldosterone dependence of ENaC in these two parts of the tubule remain unknown. One possibility is that in the CNTe, mineralocorticoid receptors are activated by glucocorticoids due to reduced activity of the 11-β-steroid dehydrogenase that protects these receptors in more distal segments. However, the enzyme is present, albeit at relatively low levels, in the DCT2 (Bostanjoglo et al., 1998). Whether these levels are sufficient to prevent illicit occupancy of mineralocorticoid receptors by corticosterone is unclear.

ROMK activities along the distal nephron

ROMK protein has been identified by immunocytochemistry in the DCT segment (Wade et al., 2011). Furthermore, ROMK channel activity in the DCT was measured using whole-cell recordings (Zhang et al., 2017; Wu et al., 2018). Here, we report a systematic study of the currents as a function of position along the distal nephron and dietary K^+ content. In the CNTe, ROMK channels were also constitutively active (Fig. 3). These currents increased with high-K and decreased with low-K food intake, changing by ∼10-fold altogether. Unlike ENaC, ROMK currents could be easily measured in the CNTas under control conditions. They increased with a high-K diet to levels similar to those in the CNTe. Although we did not measure ROMK currents in the CNT with a low-K diet, previous measurements in the rat CNT showed an ∼50% decline (Frindt et al., 2009). Thus, at least with respect to dietary K^+, regulation of ROMK appears to be similar along the K^+-secreting part of the nephron.

Our simulations suggest that the activity of ROMK channels is sufficient to explain much of K^+ secretion both under basal conditions and with increased dietary K intake. Although BK channels, likely in intercalated cells, have been shown to mediate K^+ secretion in isolated perfused collecting ducts at high flow rates (Woda et al., 2001; Carrisoza-Gaytan et al., 2020) and

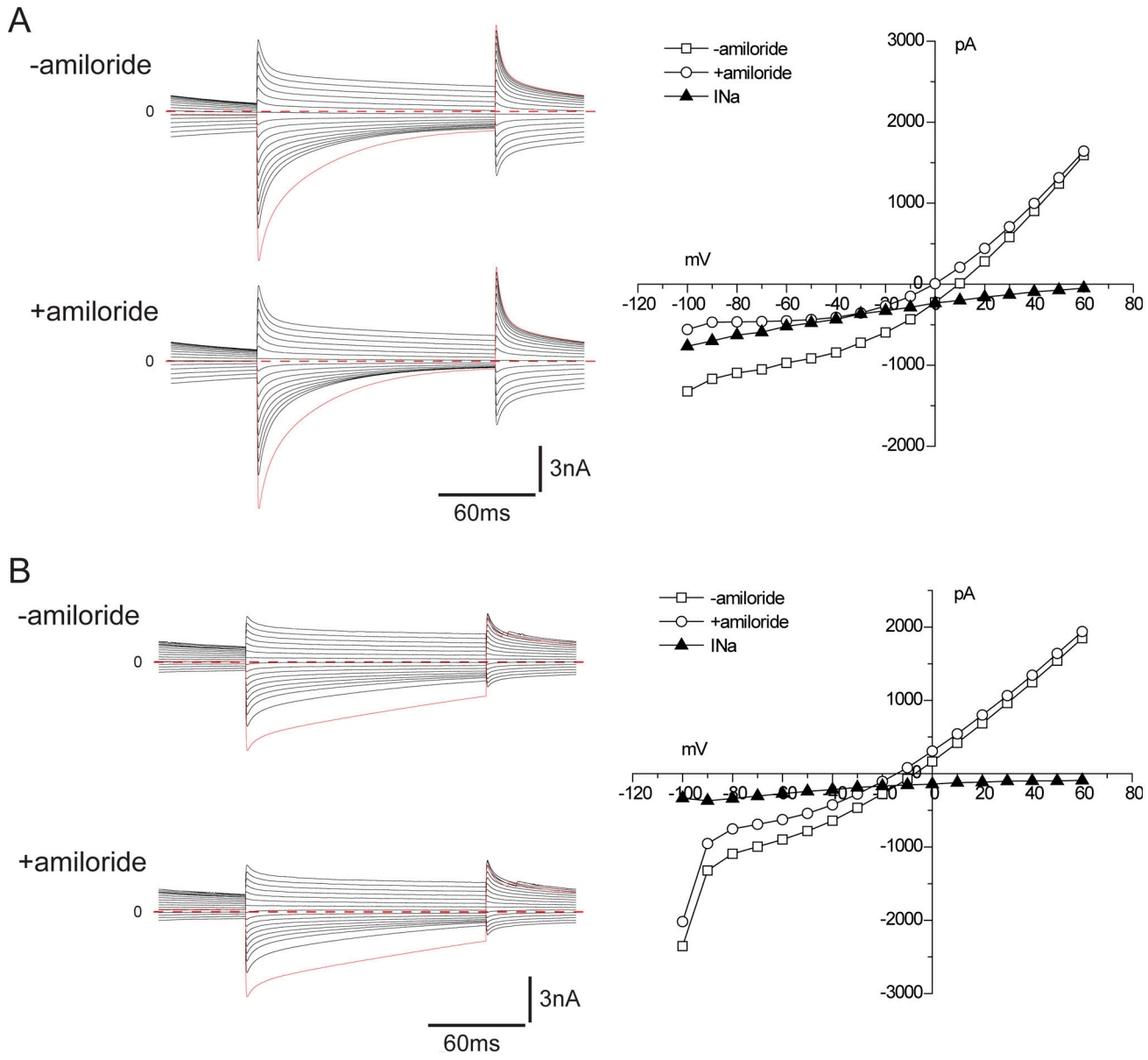

Figure 9. **ENaC current under high-K conditions.** Mice were fed a diet with 3% K for 6–8 d. Currents were measured in the presence and absence of 10 µM amiloride. Difference currents (I_{Na}) represent currents through ENaC. **(A)** Currents in a cell from region 2. **(B)** Currents in a cell from region 4.

in microperfused late DCT segments in vivo when dietary K intake is high (Bailey et al., 2006), our data indicate that they do not play a major role in determining K^+ excretion under the conditions studied. We do not know why our results differ from previous reports. These involved either in vitro recordings from isolated tubules or microperfusion of anesthetized, volume-loaded animals, while our results were obtained in vivo with conscious animals. Furthermore, our technique had limited resolution and could have missed a modest TEA-sensitive component of secretion. Our main conclusion is that ROMK channels form the predominant K^+ secretory pathway under the conditions of our studies.

Physiological significance

Having measured ENaC and ROMK in these segments, we asked to what extent these channel activities can explain K^+ secretion in vivo. In micropuncture experiments, Malnic et al. (1964) showed that the distal nephron, including the DCT and CNT, altered rates of K^+ secretion under conditions of different levels of dietary K intake and that changes in these rates could explain differences in final urinary K^+ excretion, at least with normal and high-K diets.

To assess the physiological significance of the measured activities we used a mathematical model of the rat distal nephron developed previously (Weinstein, 2005a, 2005b). Our measurements were made in mouse kidney, which is much easier to dissociate into fragments than is that of the rat. To fit our data into the rat model, we assume that channel activities per cell are similar in the two species. This assumption seems reasonable based on a comparison of the values measured in CNT in this study and in previous studies of rat CNT (Frindt and Palmer, 2004b).

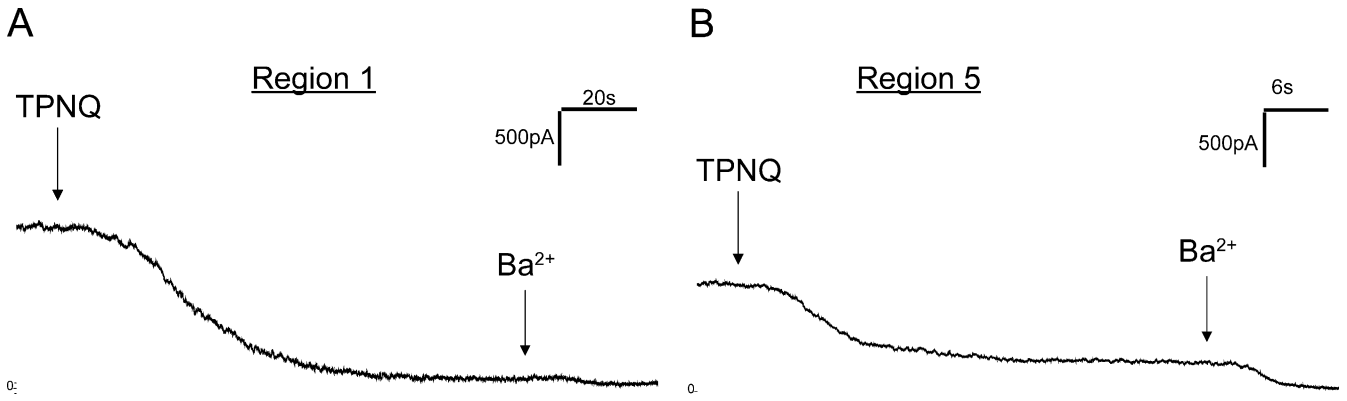

Figure 10. **ROMK current under high-K conditions.** Mice were fed a diet with 3% K for 6–8 d. Currents were measured before and after the addition of 0.1 µM TPNQ to the superfusate. Difference currents (I_{SK}) represent currents through ROMK. **(A)** Currents in a cell from region 2. **(B)** Currents in a cell from region 4.

As shown in Fig. 5, K^+ secretion through apical K^+ channels depends almost entirely on ENaC, consistent with previous modeling studies (Weinstein, 2005b; Frindt et al., 2009). Since ENaC activity is so low in the CNTas, we asked whether K^+ secretion under control conditions could be explained by transport in the CNTe. We assume that the CNTe occupies ~250 µm or the last quarter of the length of the DCT. This number has not been precisely measured, but it is in reasonable agreement with the span over which constitutive activity could be detected in the mouse distal nephron (Fig. 1). It may be longer in the rat. Using values of ENaC and ROMK permeabilities, we calculate that the CNTe adds ~9 pmol/min per tubule or ~0.65 µmol/min for the 72,000 nephrons in the two kidneys. This is close to the value of 0.8 µmol/min for amiloride-inhibitable K^+ excretion reported previously (Frindt and Palmer, 2009) for rats under similar conditions. These findings explain the observation of robust amiloride-inhibitable K^+ excretion under control conditions (Frindt and Palmer, 2009), even though ENaC activity as measured in the CCD (or late CNT) is minimal. This suggests that the CNTe can account for most of this secretion, which is in agreement with the micropuncture studies that showed little change in K^+ content between the end of the CNT and the final urine in control and K-loaded rats (Malnic et al., 1964).

When dietary K is increased, K^+ secretion continues in the CNTe and increases in the CNTas. These segments now add 16 and 28 pmol/min per nephron or 4.2 µmol/min total. This is also in fairly good agreement with the measurement of amiloride-sensitive K^+ excretion of 3 µmol/min measured in rats (Frindt and Palmer, 2009). In that study, the animals were fed a diet containing 5% K compared with 3% K in the high-K mouse chow in this study. Thus, the combination of CNTe and CNTas transport is sufficient to explain the observed ENaC-dependent K^+ excretion. It is clear, however, that the downstream CCD also responds to a high-K diet by increasing both ENaC and ROMK activities (Wang et al., 1990; Palmer et al., 1994). The physiological role of these adaptations in this segment is unclear; the enhanced K^+ secretory capacity in this segment may help to offset passive reabsorption as luminal K^+ concentrations rise. In the rat study, ~50% of K^+ excretion under high-K conditions was insensitive to amiloride. This transport is not captured in the modeling here, and its mechanism remains unknown.

Our main results are summarized in Fig. 11. Under control conditions, most K^+ secretion by the kidney occurs in the CNTe, coupled to the reabsorption of Na^+ (i.e., amiloride sensitive). When dietary K intake is increased, both ENaC activity and ROMK activity are increased in the more distal CNTas, accounting for additional Na^+-coupled K^+ secretion. With dietary K restriction, K^+ secretion in the CNTe declines but does not completely cease. The K^+ added to the urine under these conditions must be reabsorbed by a separate mechanism.

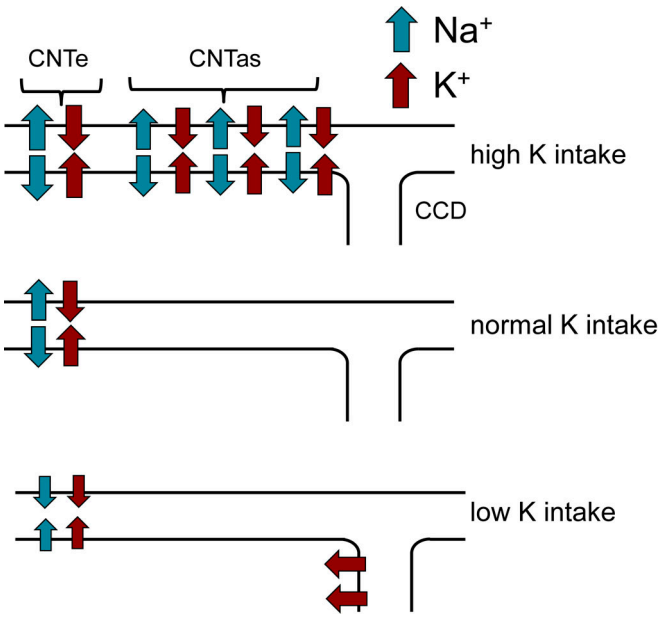

Figure 11. **Summary of urinary K^+ secretion as a function of dietary K intake.** With normal intake, secretion is restricted to the CNTe. With increased intake, more distal parts of the CNT (the CNTas) add additional K^+ to the urine. With decreased intake, secretion in the CNTe diminishes but does not stop, requiring downstream K^+ reabsorption.

Acknowledgments

Joseph A. Mindell served as editor.

We thank Prof. Johannes Loffing for the kind gift of the guinea pig anti-NCC antibody.

This work was supported by National Institutes of Health grants R01-DK111380 (to L.G. Palmer) and R01-DK29857 (to A.M. Weinstein).

The authors declare no competing financial interests.

Author contributions: L.Yang, Y. Xu, D. Gravotta, G. Frindt, and L.G. Palmer performed experimental measurements. A.M. Weinstein performed computational simulations. L.G. Palmer drafted the original version of the manuscript. All authors edited the manuscript and approved the final version.

Submitted: 1 March 2021
Accepted: 24 May 2021

References

Bailey, M.A., A. Cantone, Q. Yan, G.G. MacGregor, Q. Leng, J.B. Amorim, T. Wang, S.C. Hebert, G. Giebisch, and G. Malnic. 2006. Maxi-K channels contribute to urinary potassium excretion in the ROMK-deficient mouse model of type II Bartter's syndrome and in adaptation to a high-K diet. *Kidney Int.* 70:51–59. https://doi.org/10.1038/sj.ki.5000388

Bostanjoglo, M., W.B. Reeves, R.F. Reilly, H. Velázquez, N. Robertson, G. Litwack, P. Morsing, J. Dørup, S. Bachmann, and D.H. Ellison. 1998. 11Beta-hydroxysteroid dehydrogenase, mineralocorticoid receptor, and thiazide-sensitive Na-Cl cotransporter expression by distal tubules. *J. Am. Soc. Nephrol.* 9:1347–1358. https://doi.org/10.1681/ASN.V981347

Carrisoza-Gaytan, R., E.C. Ray, D. Flores, A.L. Marciszyn, P. Wu, L. Liu, A.R. Subramanya, W. Wang, S. Sheng, L.J. Nkashama, et al. 2020. Intercalated cell BKα subunit is required for flow-induced K+ secretion. *JCI Insight.* 5:e130553. https://doi.org/10.1172/jci.insight.130553

Cotton, C.U., A.M. Weinstein, and L. Reuss. 1989. Osmotic water permeability of Necturus gallbladder epithelium. *J. Gen. Physiol.* 93:649–679. https://doi.org/10.1085/jgp.93.4.649

Dimke, H., P. San-Cristobal, M. de Graaf, J.W. Lenders, J. Deinum, J.G. Hoenderop, and R.J. Bindels. 2011. γ-Adducin stimulates the thiazide-sensitive NaCl cotransporter. *J. Am. Soc. Nephrol.* 22:508–517. https://doi.org/10.1681/ASN.2010060606

Ergonul, Z., G. Frindt, and L.G. Palmer. 2006. Regulation of maturation and processing of ENaC subunits in the rat kidney. *Am. J. Physiol. Renal Physiol.* 291:F683–F693. https://doi.org/10.1152/ajprenal.00422.2005

Frindt, G., and L.G. Palmer. 1987. Ca-activated K channels in apical membrane of mammalian CCT, and their role in K secretion. *Am. J. Physiol.* 252: F458–F467. https://doi.org/10.1152/ajprenal.1987.252.3.F458

Frindt, G., and L.G. Palmer. 2004a. Apical potassium channels in the rat connecting tubule. *Am. J. Physiol. Renal Physiol.* 287:F1030–F1037. https://doi.org/10.1152/ajprenal.00169.2004

Frindt, G., and L.G. Palmer. 2004b. Na channels in the rat connecting tubule. *Am. J. Physiol. Renal Physiol.* 286:F669–F674. https://doi.org/10.1152/ajprenal.00381.2003

Frindt, G., and L.G. Palmer. 2009. K^+ secretion in the rat kidney: Na^+ channel-dependent and -independent mechanisms. *Am. J. Physiol. Renal Physiol.* 297:F389–F396. https://doi.org/10.1152/ajprenal.90528.2008

Frindt, G., and L.G. Palmer. 2010. Effects of dietary K on cell-surface expression of renal ion channels and transporters. *Am. J. Physiol. Renal Physiol.* 299:F890–F897. https://doi.org/10.1152/ajprenal.00323.2010

Frindt, G., A. Shah, J. Edvinsson, and L.G. Palmer. 2009. Dietary K regulates ROMK channels in connecting tubule and cortical collecting duct of rat kidney. *Am. J. Physiol. Renal Physiol.* 296:F347–F354. https://doi.org/10.1152/ajprenal.90527.2008

Garty, H., and L.G. Palmer. 1997. Epithelial sodium channels: function, structure, and regulation. *Physiol. Rev.* 77:359–396. https://doi.org/10.1152/physrev.1997.77.2.359

Jonker, J.W., E. Wagenaar, S. Van Eijl, and A.H. Schinkel. 2003. Deficiency in the organic cation transporters 1 and 2 (Oct1/Oct2 [Slc22a1/Slc22a2]) in mice abolishes renal secretion of organic cations. *Mol. Cell. Biol.* 23: 7902–7908. https://doi.org/10.1128/MCB.23.21.7902-7908.2003

Knepper, M.A., R.A. Danielson, G.M. Saidel, and R.S. Post. 1977. Quantitative analysis of renal medullary anatomy in rats and rabbits. *Kidney Int.* 12: 313–323. https://doi.org/10.1038/ki.1977.118

Lang, D.G., and A.K. Ritchie. 1990. Tetraethylammonium blockade of apamin-sensitive and insensitive Ca2(+)-activated K+ channels in a pituitary cell line. *J. Physiol.* 425:117–132. https://doi.org/10.1113/jphysiol.1990.sp018095

Loffing, J., D. Loffing-Cueni, A. Macher, S.C. Hebert, B. Olson, M.A. Knepper, B.C. Rossier, and B. Kaissling. 2000a. Localization of epithelial sodium channel and aquaporin-2 in rabbit kidney cortex. *Am. J. Physiol. Renal Physiol.* 278:F530–F539. https://doi.org/10.1152/ajprenal.2000.278.4.F530

Loffing, J., L. Pietri, F. Aregger, M. Bloch-Faure, U. Ziegler, P. Meneton, B.C. Rossier, and B. Kaissling. 2000b. Differential subcellular localization of ENaC subunits in mouse kidney in response to high- and low-Na diets. *Am. J. Physiol. Renal Physiol.* 279:F252–F258. https://doi.org/10.1152/ajprenal.2000.279.2.F252

Loffing, J., D. Loffing-Cueni, V. Valderrabano, L. Kläusli, S.C. Hebert, B.C. Rossier, J.G. Hoenderop, R.J. Bindels, and B. Kaissling. 2001a. Distribution of transcellular calcium and sodium transport pathways along mouse distal nephron. *Am. J. Physiol. Renal Physiol.* 281:F1021–F1027. https://doi.org/10.1152/ajprenal.0085.2001

Loffing, J., M. Zecevic, E. Féraille, B. Kaissling, C. Asher, B.C. Rossier, G.L. Firestone, D. Pearce, and F. Verrey. 2001b. Aldosterone induces rapid apical translocation of ENaC in early portion of renal collecting system: possible role of SGK. *Am. J. Physiol. Renal Physiol.* 280:F675–F682. https://doi.org/10.1152/ajprenal.2001.280.4.F675

Malnic, G., R.M. Klose, and G. Giebisch. 1964. Micropuncture study of renal potassium excretion in the rat. *Am. J. Physiol.* 206:674–686. https://doi.org/10.1152/ajplegacy.1964.206.4.674

Malnic, G., S. Muto, and G. Giebisch. 2008. Regulation of Potassium Excretion. *In* The Kidney. Physiology and Pathophysiology. R.J. Alpern, and S.C. Hebert, editors. Academic Press, Burlington, MA. pp. 1301–1347.

Masilamani, S., G.H. Kim, C. Mitchell, J.B. Wade, and M.A. Knepper. 1999. Aldosterone-mediated regulation of ENaC alpha, beta, and gamma subunit proteins in rat kidney. *J. Clin. Invest.* 104:R19–R23. https://doi.org/10.1172/JCI7840

Nesterov, V., A. Dahlmann, B. Krueger, M. Bertog, J. Loffing, and C. Korbmacher. 2012. Aldosterone-dependent and -independent regulation of the epithelial sodium channel (ENaC) in mouse distal nephron. *Am. J. Physiol. Renal Physiol.* 303:F1289–F1299. https://doi.org/10.1152/ajprenal.00247.2012

Palmer, L.G., and M.M. Civan. 1977. Distribution of Na+, K+ and Cl- between nucleus and cytoplasm in Chironomus salivary gland cells. *J. Membr. Biol.* 33:41–61. https://doi.org/10.1007/BF01869511

Palmer, L.G., and G. Frindt. 2006. Cl- channels of the distal nephron. *Am. J. Physiol. Renal Physiol.* 291:F1157–F1168. https://doi.org/10.1152/ajprenal.00496.2005

Palmer, L.G., L. Antonian, and G. Frindt. 1994. Regulation of apical K and Na channels and Na/K pumps in rat cortical collecting tubule by dietary K. *J. Gen. Physiol.* 104:693–710. https://doi.org/10.1085/jgp.104.4.693

Palmer, L.G., H. Sackin, and G. Frindt. 1998. Regulation of Na+ channels by luminal Na+ in rat cortical collecting tubule. *J. Physiol.* 509:151–162. https://doi.org/10.1111/j.1469-7793.1998.151bo.x

Pluznick, J.L., and S.C. Sansom. 2006. BK channels in the kidney: role in K(+) secretion and localization of molecular components. *Am. J. Physiol. Renal Physiol.* 291:F517–F529. https://doi.org/10.1152/ajprenal.00118.2006

Verrey, F., E. Hummler, L. Schild, and B.C. Rossier. 2008. Mineralocorticoid action in the aldosterone-sensitive distal nephron. *In* The Kidney: Physiology and Pathophysiology. Fourth edition. R.J. Alpern and S.C. Hebert, editors. Academic Press, Burlington, MA. 889–924.

Wade, J.B., L. Fang, R.A. Coleman, J. Liu, P.R. Grimm, T. Wang, and P.A. Welling. 2011. Differential regulation of ROMK (Kir1.1) in distal nephron segments by dietary potassium. *Am. J. Physiol. Renal Physiol.* 300: F1385–F1393. https://doi.org/10.1152/ajprenal.00592.2010

Wang, W.H., A. Schwab, and G. Giebisch. 1990. Regulation of small-conductance K^+ channel in apical membrane of rat cortical collecting tubule. *Am. J. Physiol.* 259:F494–F502. https://doi.org/10.1152/ajprenal.1990.259.3.F494

Wang, W.H., P. Yue, P. Sun, and D.H. Lin. 2010. Regulation and function of potassium channels in aldosterone-sensitive distal nephron. *Curr. Opin. Nephrol. Hypertens.* 19:463–470. https://doi.org/10.1097/MNH.0b013e32833c34ec

Weinstein, A.M. 2005a. A mathematical model of rat distal convoluted tubule. I. Cotransporter function in early DCT. *Am. J. Physiol. Renal Physiol.* 289:F699–F720. https://doi.org/10.1152/ajprenal.00043.2005

Weinstein, A.M. 2005b. A mathematical model of rat distal convoluted tubule. II. Potassium secretion along the connecting segment. *Am. J. Physiol. Renal Physiol.* 289:F721–F741. https://doi.org/10.1152/ajprenal.00044.2005

Welling, P.A. 2016. Roles and regulation of renal K channels. *Annu. Rev. Physiol.* 78:415–435. https://doi.org/10.1146/annurev-physiol-021115-105423

Woda, C.B., A. Bragin, T.R. Kleyman, and L.M. Satlin. 2001. Flow-dependent K+ secretion in the cortical collecting duct is mediated by a maxi-K channel. *Am. J. Physiol. Renal Physiol.* 280:F786–F793. https://doi.org/10.1152/ajprenal.2001.280.5.F786

Wu, P., Z.X. Gao, X.T. Su, D.H. Ellison, J. Hadchouel, J. Teulon, and W.H. Wang. 2018. Role of WNK4 and kidney-specific WNK1 in mediating the effect of high dietary K^+ intake on ROMK channel in the distal convoluted tubule. *Am. J. Physiol. Renal Physiol.* 315:F223–F230. https://doi.org/10.1152/ajprenal.00050.2018

Wu, P., Z.X. Gao, D.D. Zhang, X.P. Duan, A.S. Terker, D.H. Lin, D.H. Ellison, and W.H. Wang. 2020. Effect of angiotensin II on ENaC in the distal convoluted tubule and in the cortical collecting duct of mineralocorticoid receptor deficient mice. *J. Am. Heart Assoc.* 9:e014996. https://doi.org/10.1161/JAHA.119.014996

Yellen, G. 1984. Ionic permeation and blockade in Ca^{2+}-activated K^+ channels of bovine chromaffin cells. *J. Gen. Physiol.* 84:157–186. https://doi.org/10.1085/jgp.84.2.157

Zhang, C., L. Wang, X.T. Su, J. Zhang, D.H. Lin, and W.H. Wang. 2017. ENaC and ROMK activity are inhibited in the DCT2/CNT of TgWnk4^{PHAII} mice. *Am. J. Physiol. Renal Physiol.* 312:F682–F688. https://doi.org/10.1152/ajprenal.00420.2016

Supplemental material

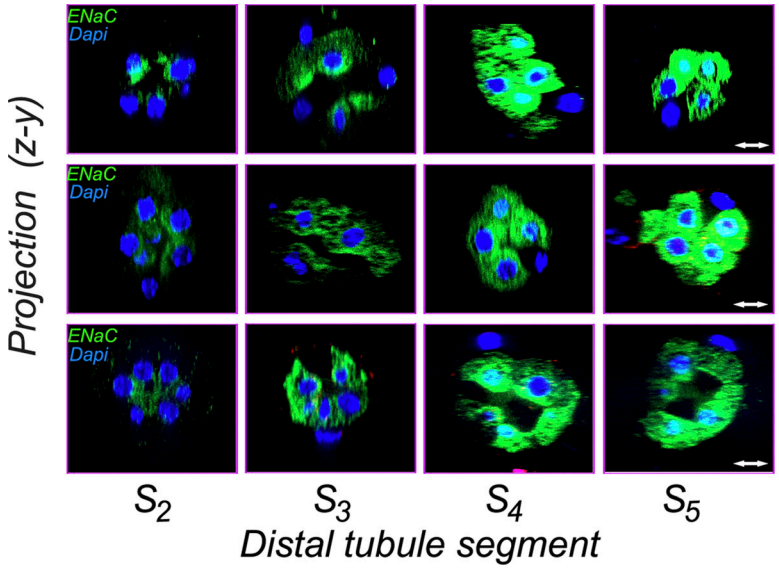

Figure S1. **Immunocytochemical localization of βENaC in segments S2–S4 of the DCT/CNT of three mice on control Na diets.** Tubules from three mice on control diet were dissected and stained with anti-βENaC antibody. Segments S2–S5 showed specific staining. In segments S2–S4, the distribution of ENaC tended to be more apical than in S5, which had a more homogenous intracellular pattern. Scale bar, 7.5 µm.